Morphology and Properties of the PA66/PC/Silicone Rubber Composites

Jun Chen, Wei Wu, Yi You, Wei Fan, Yujie Chen

Sino-German Joint Research Center of Advanced Materials, School of Materials Science and Technology, East China University of Science and Technology, Shanghai 200237, People's Republic of China

Received 23 September 2009; accepted 4 February 2010
DOI 10.1002/app.32230
Published online 27 April 2010 in Wiley InterScience (www.interscience.wiley.com).

ABSTRACT: The research focused on the PA66/PC/silicone rubber composites. By adding silicone rubber as a toughener, the composites were prepared via dynamic vulcanization. The morphology and properties of the composites were characterized by FTIR, TEM, SEM, XRD, etc. The FTIR spectrum of the composites presented an increase of the 1730, 1240, and 1450 cm^{-1} that can be due to the C═O interaction and the presence of the O─CO─O group, and this fact can mean the formation of the PA66–PC copolymer. The crosslinking of silicone rubber in the PA66/PC matrix formed the net-like structure like semi-IPN, which is propitious to enhance the interaction between PA66 matrix and PC and in further makes the PC particles embed in PA66 matrix closely. Novel composites are gained with outstanding mechanical properties and high temperature resistance, so the combine toughening by silicone rubber and PC is an ideal toughening system owing to the synergistic effect. In addition, the PA66/PC/silicone rubber/OMMT composite exhibits better flexile strength and flexile modulus without weakening other mechanical properties. © 2010 Wiley Periodicals, Inc. J Appl Polym Sci 117: 2964–2971, 2010

Key words: PA66; PC; silicon rubber; OMMT; net-like structure

INTRODUCTION

Polycarbonate (PC) is an important thermoplastic and one of the best studied is bisphenol A PC. Bisphenol A PC is an engineering thermoplastic with excellent mechanical properties, high heat distortion temperature, excellent transparency, and electrical properties, which is widely used in the fields such as electrical and electronic devices, automobiles, and construction. PC shows a high limiting oxygen index (LOI) due to relatively high tendency to charring during combustion.[1]

Silicone rubbers are notable for their following general characteristics: very wide service temperature range (−100°C to +250°C); excellent resistance to attack by oxygen, ozone, and sunlight; excellent nonstick and nonadhesive properties; low toxicity; optical transparency; good electrical insulation properties; and low chemical reactivity. However, silicone rubber has few limitations. Possible limitations include the low tensile strength of vulcanized rubbers, poor hydrocarbon oil and solvent resistance, high gas permeability, and somewhat high cost.[2]

In the past 10 years, the reactive compatibilizers have been increasingly introduced into blends.[3–8] Reactive compatibilization can also provide for a degree of control over morphology development in multiphase polymer blends via manipulation of the interfacial energies within the system,[9–11] which allowed the formation of a composite dispersed phase during a melt blending process via encapsulation of one dispersed phase by another. With chemical reaction occurring between the functional group and the blends, the interfacial adhesion would be greatly increased and the interfacial tension would be sharply decreased. However, the reactivity between functional groups was different, and the way to optimize the compatibilization was needed.

Heterogeneous blends containing polyamide 6 (PA6) have been verified by several researchers with special concern for the need to improve impact resistance.[12] The success of blend properties depends on the following three important factors: chemical reactions, physical interactions, and processing steps. Reactive blends may occur during the melt mixing processes with PA6 through hydrogen bonding.[13,14]

The compatibilization of the PA6 and PC occurs through PA6–PC block copolymer synthesized *in situ* during long melt mixing process.[12–22] The internal carbonate groups of PC may react with the amino terminal groups of PA6 during the melt mixing process at 240°C. The formation of PA6–PC copolymers suggested that these copolymers can act as compatibilizers, inducing the compatibility in the heterogeneous blends of PA6–PC.[12,15,19]

Only limited research has been pursued so far in the field of engineering plastics toughened by silicone

Correspondence to: W. Wu (wuwei@ecust.edu.cn).

© 2010 Wiley Periodicals, Inc.

rubber. There is hardly any openly published literature available in this field because of commercial sensitivity. A few research works in a related field have been patented by Dow Corning Corp.[23–25]

In this article, the PA66/PC/silicone rubber composites were developed as a kind of engineering plastics ranging from electrical power cables to other high-temperature applications. This article reports on the morphology and properties of the PA66/PC/silicone rubber composites as determined by Fourier transform infrared (FTIR), scanning electron microscopy (SEM), transmission electron microscopy (TEM), X-ray diffraction (XRD) and Torque Rheology. Toughening mechanism was studied, and the relationship between the properties and the net-like structure was also discussed at the microscales.

EXPERIMENTAL

Materials

The polyamide 6,6 was EPR27 (Shenma Nylon Engineering Plastic, Pingdingshan, China) and the PC was PC2805 (Bayer). The toughenners were additional liquid silicone rubber (two component), 8801/8802 (Shanghai Huagui Chemical Material, Shanghai, China) and methyl vinyl silicone rubber, HC 40-8110 (Dowcorning). Vulcanizing agent was benzoyl peroxide (BP) supplied by Shanghai Lingfeng Chemical additives. The filler was a natural surface-modified montmorillonite (OMMT, DK5, a nanometer montmorillonite including calcium, sodium, sodium–calcium, and magnesium smectite; the average crystal thickness is less than 25 nm, and the content of montmorillonite is higher than 95%. Zhejiang Fenghong Clay Chemicals, Anji, China.). Antioxidant agent (Irganox 1010, Ciba) and White Oil were also added as indispensable additives.

Preparation of the composites

Drying before processing was performed at 90°C in vacuum for 14 h for PA66 and PC and at 80°C in an air-circulation oven for 4 h in the case of OMMT. The PA6/PC/silicone rubber composites were obtained by dynamic vulcanization in a TE-34 corotating twin-screw extruder. The screws diameter was 34 mm and length to diameter range of the screws was 28. The barrel temperatures were 270–285°C, and the rotation speeds were 60–90 rpm. After extrusion, the extrudate was cooled in a water bath and pelletized. The formulations of PA66/PC/silicone rubber composites are presented in Table I. Subsequent injection molding was carried out in a CHEN DE CJ80M3V Plastics screw injection molding machine to obtain tensile (ISO 527-2:1993), flexile (ISO 178:1993), and impact (ISO 179-1982) specimens. The melt temperature was 275°C. The injection speed and pressure were 11.5 cm^3/s and 2300 bar, respectively.

TABLE I
The Formulations of the PA66/PC/Silicone Rubber Composites

Samples	PA66 (wt %)	PC (wt %)	Additional liquid silicone rubber (wt %)	OMMT (wt %)	Methyl vinyl silicone rubber (wt %)
1#	97	0	3	0	0
2#	93	5	2	0	0
3#	92	5	3	0	0
4#	92	5	3	1	0
5#	91	5	4	0	0
6#	91	5	0	0	4

FTIR spectra

The IR spectrum of the composites was recorded at a resolution of 4000 cm^{-1} on an IR-7685 FTIR spectrometer (Shanghai analyzer plant).

Morphology characterization

X-ray diffraction patterns were recorded in a Japan Rigaku D/max 2550VB/PC X-ray diffraction system at 40 kV/100 mA, using a Ni-filtered Cu-Ka radiation source. The scan speed was 0.58°/min. Blend morphology was examined by a JSM-6360 Keck Field Emission SEM and a Hitachi H-800 electron microscope at an acceleration voltage of 200 kV. Samples for the SEM were fractured under liquid nitrogen and then coated with Au/Pd. Samples for TEM were sectioned from molded dog bones and ultrathin-sectioned at 60–100 nm using an ultramicrotome (Reichert-Jung, ultracut E).

Mechanical characterization

Tensile testing was carried out by an SANS extensometer at a crosshead speed of 10 mm/min and at 23°C ± 2°C and 50% ± 5% relative humidity. The mechanical properties, such as tensile strength and ductility, were determined from the load–displacement curves.

Heat aging of the samples was performed for 8 h at 140°C and 6 h at 180°C by a 401-B air aging oven according to ISO 188-1998. Izod impact tests were carried out on notched specimens using a XCJ-4 4/1 J pendulum at 23°C ± 2°C and 50% ± 5% relative humidity. The notches (depth 2.54 mm and radius 0.25 mm) were machined after injection molding. A minimum of 10 impact specimens were tested for each reported value.

Rheology measurement

The melt flow rate (MFR) of the samples was obtained at 275°C with a load of 2160 g (GB3682-83) using an SRSY-1 melt flow rate tester. The torque

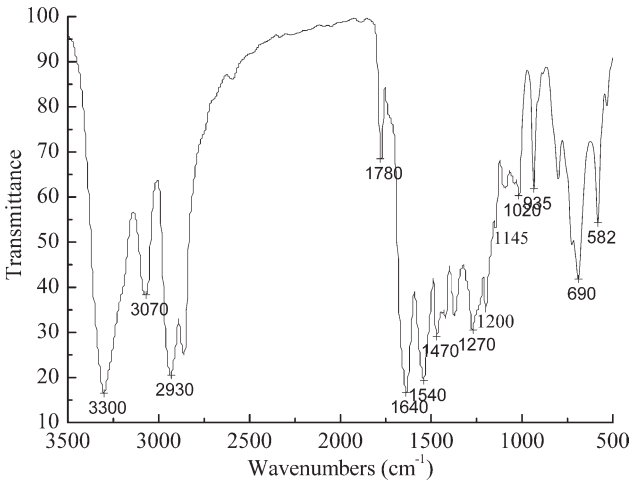

Figure 1 FTIR spectra of the PA66/PC/silicon rubber composites.

valves were measured at 275°C using a RM-200A Torque Rheometer at the speed of 20, 40, 60, and 80 rpm, respectively.

RESULTS AND DISCUSSION

FTIR spectra

FTIR spectra of the PA66/PC/silicon rubber composites are shown in Figure 1. PC shows characteristic absorption peaks at 3070, 1020, and 2930 cm^{-1} (hydrocarbonate), 1780 cm^{-1} (carbonyl C=O), and PA66 shows characteristic absorption peaks at 1640, 1540, 1200, and 935 $cm^{-1.}$ While silicone rubber (4 wt %) is characterized by a little absorption peak of Si—O at 1145 $cm^{-1.}$

Bisphenol A PC is well known to undergo transesterification reactions with a large number of polymers.[26–29] A transesterification reaction is a necessary requirement for miscibility of polyesters but requires some degree of compatibility. However, macrophase separation in blends will limit the reaction only to the interfaces. Figure 1 shows that the spectrum presented an increase of the 1730, 1240, and 1450 cm^{-1} that can be due to the C=O interaction and the presence of the O—CO—O group. This fact can mean the formation of the PA66–PC copolymer. The transesterification reaction has been found to be very slow.[30]

Generally, in polymer blends, the specific interaction between different components can result in shifting of characteristic absorption peaks for functional group in IR spectrum. With the incorporation of a small amount of silicone rubber (4 wt %), the carbonyl absorption of PC in PA66/PC/silicon rubber composites shifts to higher frequency, from 1768 cm^{-1} of pure PC to 1780 cm^{-1}. So, it can be expected that the addition of silicone rubber induces some specific interactions between phases. In this system of uncompatibilized PA66/PC blends, specific interaction may be enhanced by the addition of silicone rubber; it should be noticed that the hydrogen bonding possibly forms between silicone rubber and amino end groups in PA66 or hydroxyl end group in PC, such as O—H—O hydrogen bonding.

Morphology

Figure 2(a) is the TEM micrograph of the PA66/PC/silicone rubber composite (5#), and Figure 2(b) is the TEM micrograph of the PA66/PC/silicone rubber/OMMT composite (6#). As shown in Figure 2(a), the series of glistening droplets are just the silicone rubber particles. It can be seen that the dispersion of the silicone rubber particles as internal phase was produced by dynamic vulcanization or crosslinking within the thermoplastic organic phase and resulted in the stable droplet type morphology.

The crosslinking of silicone rubber formed the net-like structure like semi-IPN in some degree after dynamic vulcanization in the PA66/PC matrix. This

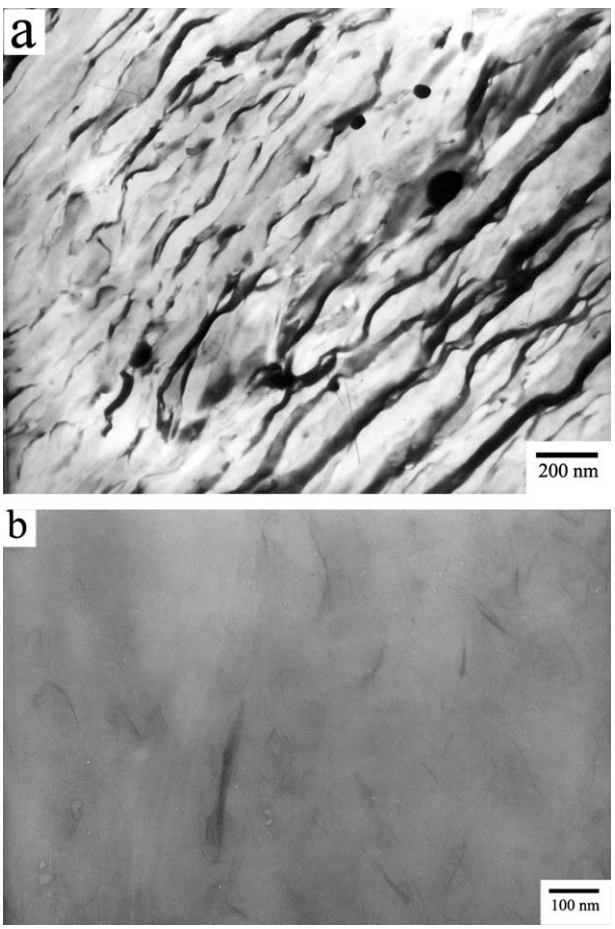

Figure 2 TEM micrographs of the PA66/PC/silicone rubber composites. (a) the PA66/PC/silicone rubber composite (5#) and (b) the PA66/PC/silicone rubber/OMMT composite (6#).

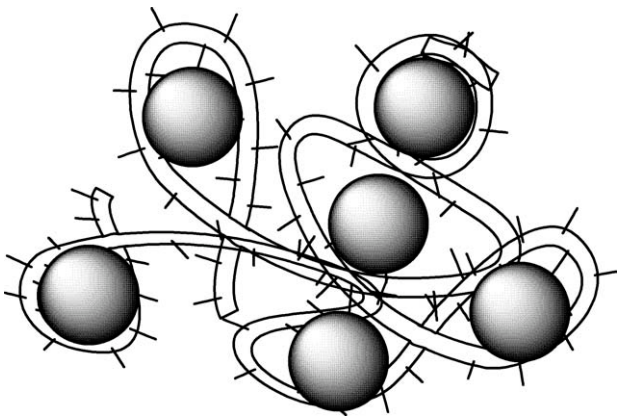

Figure 3 Schematic diagram of the net-like structures in the PA66 matrix.

net-like structure is propitious to enhance the interaction between PA66 matrix and PC and in further makes the PC particles embed in PA66 matrix closely. It is easy to imagine that the crosslinking of silicone rubber in PA66 matrix is just like a series of ropes entangled with each other to fasten the PC particles into the PA66 matrix firmly. The schematic diagram of the net-like structures in the PA66 matrix can be seen in Figure 3. Certainly, this special net-like structure is expected to exhibit enhanced properties.

Figure 4(a) is the SEM photograph of the PA66/PC alloy (95/5 wt %), and Figure 4(b) is that of the PA66/PC/silicone rubber composite (5#). It is easy to find that the PC particles become smaller and more adherent to the PA66 matrix in the PA66/PC/silicone rubber composite compared with the PA66/PC alloy. Both features confirm the compatibilizing action of the silicone rubber.

The vague interface between PA66 and PC can be attributed to the plasticization of the PA66–PC copolymer, and it is the fastening behavior of net-like structure of silicone rubber that in further improves and confirms the compatibilizing action of the PA66–PC block copolymer in the PA66/PC/silicone rubber composites.

Crystallization characterization of the composite with OMMT

Figure 5 shows the XRD patterns of pure PA66 and the PA66/PC/silicone rubber/OMMT nanocomposite samples, which was slowly cooled to room temperature naturally after being melted into thin films at 280°C. The two strong diffraction peaks at $2\Theta = 20.32°$ and 23.2° are the distinctive feature of the α phase of PA66, which are designated as α1 and α2, respectively. When adding 1 wt % OMMT, the XRD pattern still shows only the presence of the α phase; however, the intensities of the α1 and α2 peaks have changed greatly. In sharp contrast to pure PA66, the α1 diffraction peak is higher in some degree, and the

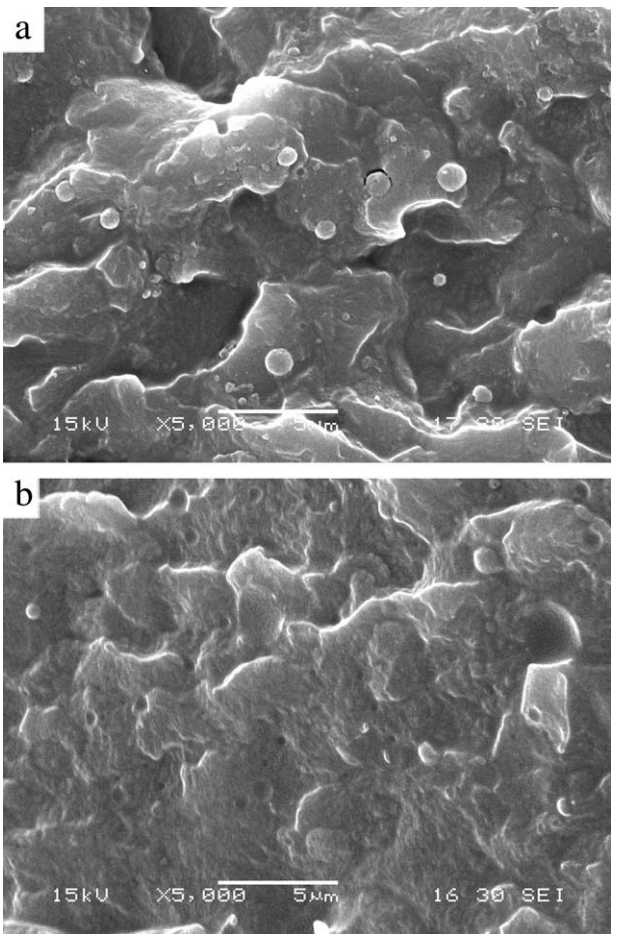

Figure 4 SEM photographs of the PA66/PC alloy and the PA66/PC/silicone rubber composite. (a) The PA66/PC alloy and (b) the PA66/PC/silicone rubber composite (5#).

α2 diffraction peak diminishes greatly in the nanocomposite, which indicates that the addition of OMMT changes the structure of the α crystal phase.

The α phase consisted of planar sheets of hydrogen bonding chains with sheets stacked upon one

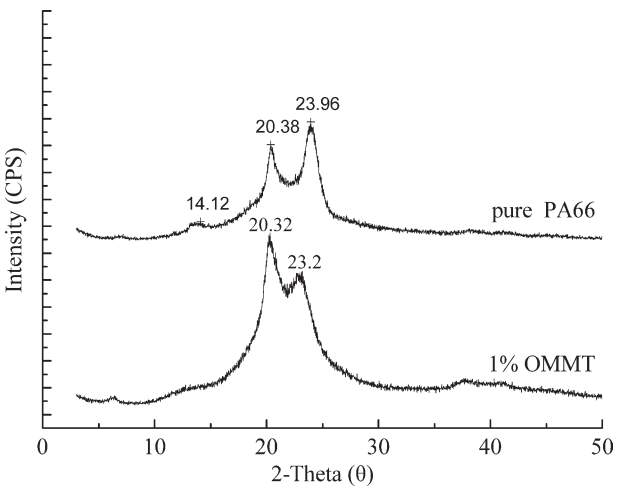

Figure 5 XRD patterns of pure PA66 and the PA66/PC/silicone rubber/OMMT nanocomposite samples.

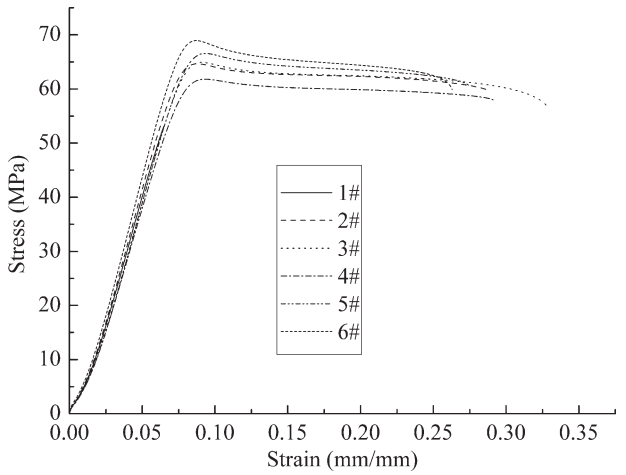

Figure 6 The tensile stress/strain curves of the PA66/PC/silicone rubber composites.

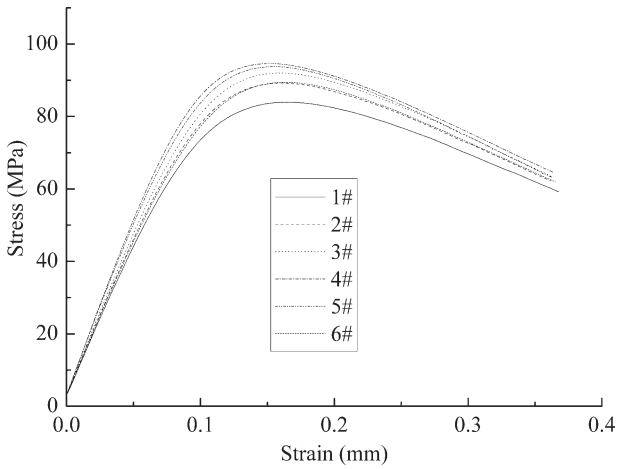

Figure 7 The flexile stress/strain curves of the PA66/PC/silicone rubber composites.

another and displaced along the chain direction by a fixed amount.[31–34] The sharp decrease in intensity of the α2 peak in the nanocomposite indicates that the addition of OMMT disturbs the perfect arrangement of hydrogen-bonded sheets of the α phase. In common, the characteristic of the γ phase in PA66 is two diffraction peaks at $2\Theta = 21.7^\circ$ and 13.6°, respectively. As the α phase is much more thermodynamically stable than γ phase of PA66 at room temperature,[34] the introduction of silicate layers still has not brought the appearance of γ phase in PA66.

In addition, no visible diffraction peak normally for OMMT at small angles from 3° to 10° in XRD pattern above is found, which could be attributed to the formation of swollen and disordered intercalated tactoids or the exfoliation of OMMT. As the incorporated amount of PC and silicone rubber was limited, leading to no extra observable diffraction peaks for the blends, no clear effect of silicone rubber on the crystalline structure of nanocomposite has been observed.

Tensile and flexile properties

The mechanical properties of PA66/PC/silicone rubber composites are presented in Figures 6, 7, and Table II. As shown in Table II, the tensile properties become better whatever for tensile strength, yield stress, maximal stress, or elongation at break with the increasing loading of liquid silicone rubber. From the phenomenon that the composite without PC (1#) becomes failure even before yielding during tensile testing, it can be seen that PC makes big contribution on tensile strength of the PA66/PC/silicone rubber composites.

The composite containing methyl vinyl silicone rubber (6#) exhibits better tensile properties compared with the composites containing liquid silicone rubber, which may attribute to the part deactivation of platinum catalyst for liquid silicone rubber because of the inhibitory effect of amide group of PA66 in high-temperature atmosphere and in further decreasing the level of dynamic vulcanization.

From the flexile curves of the PA66/PC/silicone rubber composites shown in Figure 7, it can also be found that flexile strength and flexile modulus of the composites become bigger with the increasing loading of liquid silicone rubber. Contrary to the tensile testing result, the flexile strength of composites containing liquid silicone rubber is better than the composite containing methyl vinyl silicone rubber (6#).

Impact behavior before and after heat aging

Figure 8 shows the comparison of impact strength for the PA66/PC/silicone rubber composites after heat

TABLE II
The Data of Mechanical Properties for the PA66/PC/Silicone Rubber Composites

Samples	Tensile strength (MPa)	Tensile modulus (GPa)	Elongation at break (%)	Maximal stress (KN)	Flexile strength (MPa)	Flexile modulus (MPa)
1#	53.36	0.39	6.52	2.12	84.01	2159.70
2#	64.58	0.47	29.03	2.50	89.28	2279.24
3#	65.59	0.54	28.49	2.52	92.07	2350.21
4#	63.48	0.42	30.66	2.46	94.66	2540.53
5#	67.05	0.44	31.64	2.53	93.84	2561.70
6#	68.96	0.55	26.94	2.65	89.515	2205.15

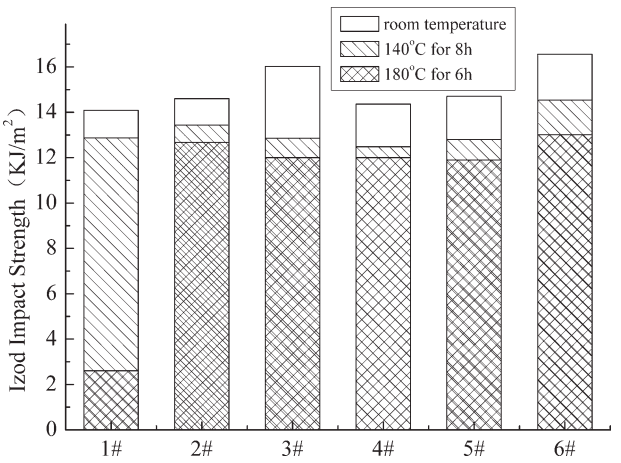

Figure 8 The impact strength comparison of the PA66/PC/silicone rubber composites after heat aging at different temperatures.

aging at different temperatures. From the comparison of impact strength at room temperature, it can be found that the impact strength of the composites becomes larger with the increasing loading of liquid silicone rubber. The net-like structure formed by the crosslinking of silicone rubber in PA66/PC matrix can transfer the impact energy to the droplet particles of silicone rubber, which can absorb the impact energy in the largest degree. At the same time, the PC particles fastened by the net-like structure can supply enough stiffness for the composites. Therefore, the combine toughening by silicone rubber and PC can be said an ideal toughening system because of the synergistic effect. The phenomenon that the PA66/PC/silicone rubber composites have higher impact strength compared with the composite without PC (1#) indicates that the introduction of PC makes big contribution on impact strength of the composites.

From the comparison of impact strength after heat aging at different temperatures (Fig. 8), it can be found that the impact strength of all the composites after 8 h at 140°C is a little lower than that of the original samples at room temperature; as for the situation after 6 h at 180°C, all the samples have a slight decrease on impact strength except the PA66/silicone rubber composites (1#), which has a sharp decline on impact strength. That fully exhibits the high temperature resistance of PC, which can be continuously used at 120–150°C, and still maintain the outstanding mechanical properties. Altogether, the PA66/PC/silicone rubber composites show very good retention of properties even after heat aging, and this indicates good resistance to heat.

In the PA66/PC/silicone rubber composites, PA66 as partially crystalline polymers with originally ductile characteristics, loss of Izod impact strength in the course of heat aging is the result of molecular degradation caused by C—C chain scission mechanism of thermooxidation, leading to the reduction of molecular weight and the crystal size of the polymer matrix, in further the transition from ductile to brittle behavior. Additionally, this mechanical properties failure is also associated with microcrack formation on the phase interface between PA66 and PC in the matrix because of diffusion-controlled aging. Crack formation starts from oxidized, brittle surface, and subsequent propagates into the ductile material under mechanical stress.[35–38]

Compared with the additional liquid silicone rubber (two component), the composite containing methyl vinyl silicone rubber (6#) exhibits the highest impact strength before or after heat aging, which is ascribed to peroxide curing providing strong C—C linkages as crosslinking.

Role of OMMT

The PA66/PC/silicone rubber/OMMT composite (4#) exhibits better flexile strength and flexile modulus (Table II) without the weakening of other mechanical properties compared with the composites without OMMT.

A driving force for the exfoliation of the silicate layers of OMMT should come at least partly from the interaction between the silicate layers and the silicone rubber in the PA66/PC matrix, because of the participation of the silanol groups of OMMT during the preparation of the PA66/PC/silicone rubber/OMMT composite and the hybrid formation of OMMT tethered with silicone rubber molecules. If the silanol groups of OMMT participated in the vulcanizing crosslinking process, OMMT can act as active sites to increase crosslinking degree and lead to denser net-like structure of the nanocomposite. Therefore, the silicate layers of OMMT crosslinked in the net-like structure can support enough stiffness for composite just like the steel bars in concrete building.

The impact strength of the PA66/PC/silicone rubber/OMMT composite (4#) decreases a little with the introduction of OMMT (1 wt %), which can also be indicated by the phenomenon that the Izod impact strength value is the area under a force–displacement curve. The addition of OMMT reduces the extent of plastic deformation, that is, reduces the area under a force–displacement curve, at least in tensile tests as shown in Figure 6.

The role of OMMT in the nanocomposite can be related to the parameters such as the bound silicone rubber (the net-like structure of silicone rubber restricted by silicate layers), silicone rubber shell creation (voids in the silicone rubber) in the vicinity of silicate layers,[39] the small agglomerates of OMMT on the interface between PA66 and PC, and occlusion of PA66 within the clay galleries.

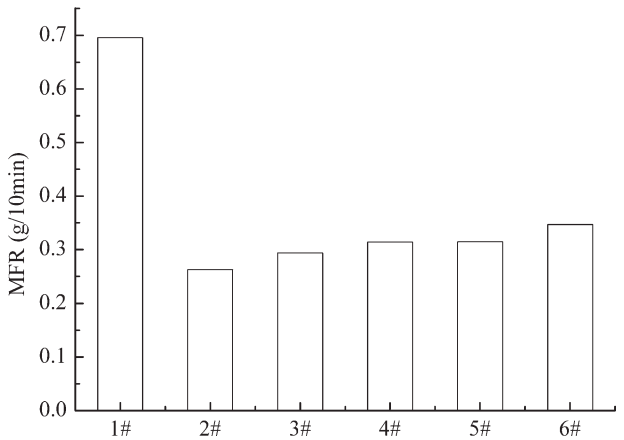

Figure 9 The comparison of melt flow rate (MFR) valves for the PA66/PC/silicone rubber composites.

In the composites without OMMT, numerous voids (subcritical cracks) appeared in silicone rubber particles dispersed in the PA66/PC matrix during drawing, and cracks were generated via voiding with the input energy dissipated (e.g., by conversion into heat). The toughening mechanism of the PA66/PC/silicone rubber/OMMT composite (4#) was assumed to be platelet orientation, chain slippage, and zigzag energy dissipation. The nanoeffect of the silicate layers could restrict the movement of polymer chains and combine them with silicate layers. This may have reduced the number or size of voids of silicone rubber in their vicinity and the energy dissipating in further. While increase in the crack path around the silicate layers (zigzag route) could also be considered a mechanism of energy dissipation. By this suggested model, the toughening mechanism is more complicated for this nanocomposite, and the impact strength has a little decline by the introduction of OMMT.

Rheology properties

Figure 9 shows the comparison of MFR valves for the PA66/PC/silicone rubber composites. It is interesting to note that the MFR value of composite is a little bigger with the increasing loading of silicone rubber. In common the introduction of rubber is unfavorable for the processability of composite, while silicone rubber can be a flowability modifier for plastics as it contains —Si—O—R— group. As for the introduction of PC, it can be observed that the MFI valves of the composite without PC (1#) exhibit the best fluidness, which should attribute to the higher viscosity of PC in the composites.

Torque valves versus rotation speed for the PA66/PC/silicone rubber composites are presented in Figure 10. It can be observed that the torque valves for all the composites increase gradually with the increasing of rotation speed. In addition, the torque valve is bigger in low-rotation speed zone and smaller conversely in high-rotation speed zone for the higher loading of liquid silicone rubber in the PA66/PC matrix (2#, 3#, 5#).

The relationship between the torque valves of the composites and rotation speed can be explained by the net-like structure theory of the composites. When the melt temperature reaches the melting point of the composites in the Torque Rheometer, the net-like structure of the composites begins to be destroyed continuously. At the same time, the liquid silicone rubber in the PA66/PC matrix begins to experience the new course of dynamic vulcanization and formed the new net-like structure because of the residue of the vulcanization agent. Therefore, it is in a continuous dynamic balance between disintegration and reconstruction for the net-like structure of the composites. In low-rotation speed zone, the net-like structure can be reconstructed in time, which sustains the density of the net-like structure, so the acceleration of the torque valves for the composites is stable. While in high-rotation speed zone, the destroying speed of the crosslinking points is beyond the reconstructing speed; the acceleration of the viscosity versus shear rate begins to decline, especially for the high loading of silicone rubber in the PA66/PC/silicone rubber composites with a high crosslinking degree, so the torques valves of the composites with a high loading of silicone rubber are a little lower than that of the composites with a low loading of silicone rubber in high-rotation speed zone.

As for the PA66/PC/silicone rubber/OMMT composites (4#), it is obvious that the introduction of OMMT makes the viscosity of the composites higher whatever the rotation speed is, certainly this is because the silicate layers of OMMT do not melt at the melting point of the composite and become so

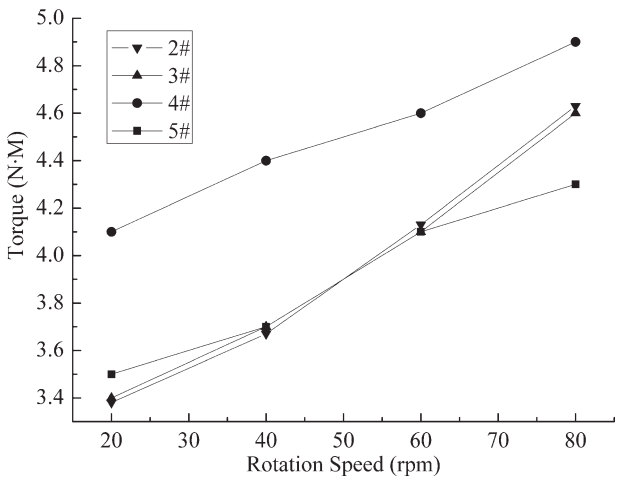

Figure 10 Torque valves versus rotation speed for the PA66/PC/silicone rubber composites.

many small obstacles in the melt flow of the composites.

CONCLUSIONS

The PA66/PC/silicone rubber composites can become an outstanding engineering plastics with good high temperature resistance. The FTIR spectrum of the composites presented an increase of the 1730, 1240, and 1450 cm^{-1} that can be due to the C═O interaction and the presence of the O─CO─O group. This fact can mean the formation of the PA66–PC copolymer. The crosslinking of silicone rubber formed the net-like structure like semi-IPN in some degree after dynamic vulcanization in the PA66/PC matrix. This net-like structure is propitious to enhance the interaction between PA66 matrix and PC and in further makes the PC particles embed in PA66 matrix closely. The vague interface between PA66 and PC can be attributed to the plasticization of the PA6–PC copolymer, and it is the fastening behavior of net-like structure of silicone rubber that in further improves and confirms the compatibilizing action of the PA6–PC block copolymer in the PA66/PC/silicone rubber composites. The tensile properties become better whatever for tensile strength, yield stress, maximal stress, or elongation at break with the increasing loading of liquid silicone rubber, the same for flexile strength and flexile modulus. The net-like structure formed by the crosslinking of silicone rubber in PA66/PC matrix can transfer the impact energy to the droplet particles of silicone rubber, which can absorb the impact energy in the largest degree. At the same time, the PC particles fastened by the net-like structure can supply enough stiffness for the composites. Therefore, the combine toughening by silicone rubber and PC can be said an ideal toughening system because of the synergistic effect. Furthermore, the composites show very good retention of impact strength even after heat aging. As for the PA66/PC/silicone rubber/OMMT nanocomposite (4#), the $\alpha 1$ diffraction peak is higher in some degree and the $\alpha 2$ diffraction peak diminishes greatly in sharp contrast to pure PA66, which indicates that the addition of OMMT changes the structure of the α crystal phase. The nanocomposite exhibits better flexile strength and flexile modulus without the weakening of other mechanical properties compared with the composites without OMMT.

References

1. Dong, Q.-X.; Chen, Q.-J.; Yang, W.; Zheng, Y.-L.; Liu, X.; Li, Y.-L.; Yang, M.-B. J Appl Polym Sci 2008, 109, 659.
2. Basuli, U.; Chaki, T. K.; Naskar, K. J Appl Polym Sci 2008, 108, 1079.
3. Machado, J. M.; Lee, C. S. Polym Eng Sci 1994, 34, 59.
4. Kim, J. K.; Kim, S.; Park, C. E. Polymer 1997, 38, 2155.
5. Al-Malaika, S.; Kong, W. J Appl Polym Sci 2001, 79, 1401.
6. Wilkinson, A. N.; Clemens, M. L.; Harding, V. M. Polymer 2004, 45, 5239.
7. Al-Malaika, S.; Kong, W. Polymer 2005, 46, 209.
8. Cheng, T. W.; Keskkula, H.; Paul, D. R. Polymer 1992, 33, 1606.
9. Guo, H. F.; Packirisamy, S.; Gvozdic, N. V.; Meier, D. J. Polymer 1997, 38, 785.
10. Guo, H. F.; Gvozdic, N. V.; Meier, D. J. Polymer 1997, 38, 4915.
11. Reignier, J.; Favis, B. D.; Heuzey, M. C. Polymer 2003, 44, 49.
12. Gattiglia, E.; Turturro, A.; Pedemonte, E.; Dondero, G. J Appl Polym Sci 1990, 41, 1411.
13. Jannasch, P.; Wesslen, B. J Appl Polym Sci 1995, 58, 753.
14. Huang, M. W.; Zhu, K. J.; Pearce, E. M.; Kwei, T. K. J Appl Polym Sci 1993, 48, 563.
15. Montaudo, G.; Puglisi, C.; Samperi, F.; Lamantia, F. P. J Polym Sci Part A: Polym Chem 1996, 34, 1283.
16. Gattiglia, E.; Turturro, A.; Pedemonte, E. J Appl Polym Sci 1989, 38, 1807.
17. Gattiglia, E.; La Mantia, F. P.; Turturro, A.; Valenza, A. Polym Bull 1989, 21, 47.
18. Eguiazábal, J. I.; Nazábal, J. Makromol Chem Symp 1988, 20, 255.
19. Gattiglia, E.; Turturro, A.; La Mantia, F. P.; Valenza, A. J Appl Polym Sci 1992, 46, 1887.
20. Kim, W.; Park, C.; Burns, C. M. J Appl Polym Sci 1993, 49, 1003.
21. Montaudo, G.; Puglisi, C.; Samperi, F. J Polym Sci Part A: Polym Chem 1994, 32, 15.
22. Tavares, M. I. B.; Castro, W. P.; Costa, D. A. J Appl Polym Sci 1995, 55, 1165.
23. Gornowicz, G. A.; Lupton, K. E.; Romenesko, D. J.; Struble, K.; Zhang, H. (to Dow Corning Corp.). U.S. Pat. 6,013,715 (2000).
24. Gornowicz, G. A. (to Dow Corning Corp.). U.S. Pat. 6,015,858 (2000).
25. Gornowicz, G. A.; Zhang, H. (to Dow Corning Corp.). U.S. Pat. 6,153,691 (2000).
26. Li, M.-S.; Ma, C.-C.; Chang, F. C. Polymer 1997, 38, 855.
27. Mondragon, I.; Gaztelamendi, M.; Nazabal, J. Polym Eng Sci 1986, 26, 1478.
28. Montaudo, G.; Puglisi, C.; Samperi, F. J Polym Sci Part A: Polym Chem 1993, 31, 13.
29. Ishida, H.; Lee, Y.-H. J Appl Polym Sci 2002, 83, 1848.
30. Berty, C.; Bonora, V.; Pilati, F.; Fiorini, M. Macromol Chem 1992, 193, 1679.
31. Kyotani, M.; Mitsuhashi, S. J Polym Sci Part A-2: Polym Phys 1972, 10, 1497.
32. Abu-Isa, I. J Polym Sci Part A-1:Polym Chem 1971, 9, 199.
33. Hiramatsu, N.; Hirakawa, S. Polym J 1982, 14, 165.
34. Dasgupta, S.; Hammond, W. B.; Goddard, W. A. J Am Chem Soc 1996, 118, 12291.
35. Zweifel, H. Stabilization of Polymeric Materials; Springer Verlag: Berlin, 1998; p 18.
36. Gugumus, F. In Developments in Polymer Stabilization—8; Scott, G., Ed.; Elsevier Applied Science Publishers: London, 1987; p 239.
37. Factor, A.; Ligon, W. V.; May, R. J. Macromolecules 1987, 20, 2462.
38. Gugumus, F. Polym Degrad Stab 1998, 62, 245.
39. Wang, J.; Chen, Y. J Appl Polym Sci 2008, 107, 2059.